Available online at www.sciencedirect.com

ScienceDirect

Journal of Molecular Structure 876 (2008) 102–109

Journal of
MOLECULAR
STRUCTURE

www.elsevier.com/locate/molstruc

Photoinduced intramolecular charge-transfer state in thiophene-π-conjugated donor–acceptor molecules

Ruikui Chen [a], Guangjiu Zhao [b], Xichuan Yang [a,*], Xiao Jiang [a], Jifeng Liu [b], Haining Tian [a], Yan Gao [a], Xien Liu [a], Keli Han [b,*], Mengtao Sun [c], Licheng Sun [a,d,*]

[a] *State Key Laboratory of Fine Chemicals, DUT-KTH Joint Education and Research Center on Molecular Devices, Dalian University of Technology (DUT), Zhongshan Road 158-46, 116012 Dalian, PR China*
[b] *Dalian Institute of Chemical Physics, Chinese Academy of Sciences, Zhongshan Road 457, 116023 Dalian, PR China*
[c] *National Laboratory for Condensed State Matter Physics, Institute of Physics, Chinese Academy of Sciences, P.O. Box 603-146, 100080 Beijing, PR China*
[d] *Center of Molecular Devices, Department of Chemistry, Organic Chemistry, Royal Institute of Technology (KTH), Teknikringen 30, 10044 Stockholm, Sweden*

Received 5 March 2007; received in revised form 29 May 2007; accepted 30 May 2007
Available online 21 June 2007

Abstract

Novel thiophene-π-conjugated donor–acceptor molecules, 5-[2-(1,2,2,4-tetramethyl-1,2,3,4-tetrahydroquinolin-6-yl)-vinyl]-thiophene-2-carbaldehyde (**QTC**) and (1-cyano-2-{5-[2-(1,2,2,4-tetramethyl-1,2,3,4-tetrahydroquinolin-6-yl)-vinyl]-thiophen-2-yl}-vinyl)-phosphonic acid diethyl ester (**QTCP**), were designed and synthesized. Combined experimental and theoretical methods were performed to investigate the photoinduced intramolecular charge-transfer (ICT) processes of these compounds. Steady-state absorption and fluorescence measurements in different solvents indicate the photoinduced ICT characters of **QTC** and **QTCP**. Solvent dependency of the large Stokes shifts and high dipole moment of the excited state also support the charge-transfer character of the excited state. Theoretical calculations based on time-dependent density functional theory (TDDFT) method were performed to investigate ICT states of these compounds. The results reveal that the excited states have adopted a distortion of the C=C double bond between the donor moiety and the thiophene-π-bridge.

Keywords: Intramolecular charge transfer; Donor-π-acceptor; Tetrahydroquinoline; Thiophene; Time-dependent density functional theory

1. Introduction

The electron donor–acceptor π-conjugated (D-π-A) compounds have been recognized as target compounds for numerous applications in material science range, such as nonlinear optical materials [1,2], electrogenerated chemiluminescence materials [3,4], fluorescence probes [5,6] and dye-sensitized solar cells [7]. The photoinduced intramolecular charge-transfer (ICT) character of the excited state in these D-π-A compounds is key to their outstanding optical and electronic properties [8,9]. Thus, characterization of the ICT state (e.g., electronic nature and molecular geometry) will give deep insight into the relationship between molecular structures and properties.

The phenomenon of dual fluorescence, discovered by Lippert et al. [10,11] 40 years ago, in compound 4-(*N*,*N*-dimethylamino) benzonitrile (DMABN), is an example of ICT fluorescence of D-π-A compound, which has led to numerous theoretical and experimental studies to account for the origin of ICT fluorescence [10–25]. However, even for DMABN, the structure of ICT state is still amphibolous [14,20]. Several distinct models, especially for the twisted intramolecular charge transfer (TICT) [12–18] and planar intramolecular charge transfer (PICT) [19–21],

---

* Corresponding authors. Tel.: +86 411 88993886, fax: +86 411 83702185 (X.Yang); tel.: +86 411 84379293, fax: +86 411 84675584 (K. Han); tel.: +46 8 7908127, fax: +46 8 7912333 (L. Sun).
E-mail addresses: yangxc@dlut.edu.cn (X. Yang), klhan@dicp.ac.cn (K. Han), lichengs@kth.se (L. Sun).

0022-2860/$ - see front matter © 2007 Elsevier B.V. All rights reserved.
doi:10.1016/j.molstruc.2007.05.045

have been proposed to explain the formation and the final structure of the ICT state. Although some direct experimental proofs of excited-state structures have been obtained by picosecond X-ray diffraction [26], transient infrared spectroscopy [27] and laser-induced fluorescence excitation spectroscopy [28,29] technologies, it's also difficult to determine the ICT excited-state geometry for most cases. In recent years, theoretical calculations are employed to interpret the properties of various donor–acceptor substituted systems [30–32]. It is found that the theoretical analysis is an appropriate technique to get insight into the characters of the ground and excited states, as well as the mechanism of the ICT processes [16–18,22–25].

In this study, we report the combined experimental and theoretical studies on the ICT processes in thiophene-π-conjugated donor–acceptor molecules, 5-[2-(1,2,2,4-tetramethyl-1,2,3,4-tetrahydroquinolin-6-yl)-vinyl]-thiophene-2-carbaldehyde (**QTC**) and (1-cyano-2-{5-[2-(1,2,2,4-tetramethyl-1,2,3,4-tetrahydroquinolin-6-yl)-vinyl]-thiophen-2-yl}-vinyl)-phosphonic acid diethyl ester (**QTCP**) (Scheme 1). The 1,2,2,4-tetramethyl-1,2,3,4-tetrahydroquinoline (TMTHQ) moiety with strong electron donating ability has been synthesized to construct push–pull charge-transfer complexes [33]. Furthermore, the tertiary amino group fixed by the six member ring in TMTHQ makes the electron donor moiety more rigid and will decrease the complexity of structural changes in the discussion of the excited-state geometries below. The five-membered heteroaromatic compound thiophene has also been employed as the conjugating units on designing novel push–pull structures, since thiophene has lower delocalization energy than benzene, it can offer a more effective conjugation in donor–acceptor compounds [34]. In a previous study, we have reported the electrogenerated chemiluminescence property of **QTCP** and other analogs, indicating the potential applications of these type compounds [35]. Herein, the details of synthesis of **QTC** and **QTCP** are reported. Systematic studies on the electronic spectra of **QTC** and **QTCP** have been carried out and suggested a strong photoinduced ICT character of the excited state. Moreover, theoretical calculations based on time-dependent density functional theory (TDDFT) method were performed to get insight into the charge-transfer excited-state properties. The results reveal that the excited state has adopted a distortion of the C=C double bond between the donor moiety and the thiophene-π-bridge.

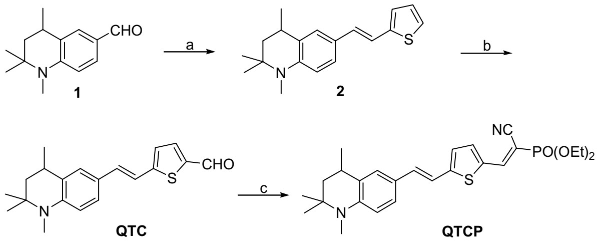

Scheme 1. Chemical structures and synthetic route of the D-π-A molecules. (a) *t*-BuOK, diethyl 2-thienylmethylphosphonate, THF, 0 °C, 2 h, 95 %; (b) *n*-BuLi, DMF, THF, −15 °C, 56%; (c) diethyl cyanomethylphosphonate, CH_3CN, piperidine, reflux, 2 h, 78%.

2. Experiment details

2.1. Material

The investigated **QTC** and **QTCP** were synthesized based on several classical procedures and the synthetic route is shown in Scheme 1. 6-Formyl-1,2,2,4-tetramethyl-1,2,3,4-tetrahydroquinoline (**1**) was obtained using improved literature procedures [33,36]. Reaction of **1** with diethyl 2-thienylmethylphosphonate in the presence of *t*-BuOK via Wittig–Horner conditions led to the formation of compound **2**. Formylation reaction of **2** by *n*-BuLi/DMF yielded **QTC**. The Knoevenagel condensation of **QTC** with diethyl cyanomethyl-phosphonate in the presence of piperidine gave **QTCP**. The purities and structures of the intermediates and target compounds were characterized by thin layer chromatography (TLC), elemental analysis, ^{1}H NMR and high resolution mass spectra.

2.1.1. 1,2,2,4-Tetramethyl-6-(2-thiphen-2-yl-vinyl)-1,2,3,4-tetrahydro-quinoline (2)

To a solution of *t*-BuOK (353 mg, 3.15 mmol) in 10 mL fresh distilled THF, diethyl 2-thienylmethylphosphonate (725 mg, 3.1 mmol) was added dropwise at 0 °C under protection of N_2. The mixture was vigorously stirred in an ice bath. Then **1** (545 mg, 2.5 mmol) in 10 mL anhydrated THF was added dropwise in about 30 min and stirring was continued for 2 h. After removing the solvent, the residue was loaded on column chromatography (silica gel, CH_2Cl_2 as eluent). The desired product was obtained as a yellow solid (706 mg, 95%). Mp. 87–89 °C. 1H NMR (Acetone-d_6, 400 MHz, ppm): δ 1.21 (s, 3H), 1.30 (s, 3H), 1.36 (d, $J = 6.7$ Hz, 3H), 1.46 (dd, $J_1 = 12.7$ Hz, $J_2 = 13.0$ Hz, 1H), 1.85 (dd, $J_1 = 4.5$ Hz, $J_2 = 12.9$ Hz, 1H), 2.84 (s, 3H), 2.80–2.87 (m, 1H), 6.56 (d, $J = 8.5$ Hz, 1H), 6.88 (d, $J = 16.0$ Hz, 1H), 6.99 (dd, $J_1 = 3.5$ Hz, $J_2 = 5.1$ Hz, 1H), 7.04 (d, $J = 3.5$ Hz, 1H), 7.15 (d, $J = 16.1$ Hz, 1H), 7.23–7.24 (m, 2H), 7.31 (s, 1H). HRMS-EI (*m*/*z*): $[M]^+$ calcd for $C_{19}H_{23}NS$, 297.1551; found, 297.1546; Anal. calcd for $C_{19}H_{22}NS$: C 76.72, H 7.79, N 4.71; found C 76.51, H 7.82, N 4.52.

2.1.2. 5-[2-(1,2,2,4-Tetramethyl-1,2,3,4-tetrahydro-quinolin-6-yl)-vinyl]-thiophene-2-carbaldehyde (QTC)

A solution of *n*-BuLi in hexane (2.57 M, 0.43 mL, 1.1 mmol) was added dropwise to a solution of **2** (297 mg, 1 mmol) in anhydrated THF (20 mL) at −15 °C under N_2 protection. Then the mixture was stirred for another 20 min at −15 °C. Anhydrous DMF (0.09 mL, 1.2 mmol) was added to the above reaction mixture. After stirring at −15 °C for 2 h, the reaction mixture was poured into 50 mL of ice water. After extracted three times by CH_2Cl_2, the extraction was dried on magnesium sulfate and removed of solvent. The residue was subjected to column chromatography (silica gel, CH_2Cl_2 as the eluent), 182 mg (56%) of red-brown solid was obtained. Mp 138–139 °C. ^1H NMR (Acetone-d_6, 400 MHz, ppm): δ 1.24 (s, 3H), 1.32 (s, 3H), 1.37 (d, $J = 6.6$ Hz, 3H), 1.47 (dd, $J_1 = 12.7$ Hz, $J_2 = 2.9$ Hz, 1H), 1.87 (dd, $J_1 = 4.4$ Hz, $J_2 = 13.0$ Hz, 1H), 2.88 (s, 3H), 2.79–2.85 (m, 1H), 6.59 (d, $J = 8.6$ Hz, 1H), 7.20–7.22 (m, 3H), 7.33 (dd, $J_1 = 1.7$ Hz, $J_2 = 8.5$ Hz, 1H), 7.39 (s, 1H), 7.82 (d, $J = 3.9$ Hz, 1H), 9.85 (s, 1H); HRMS-EI (*m/z*): $[M]^+$ calcd for $C_{20}H_{23}NOS$, 325.1500; found, 325.1500.; Anal. calcd for $C_{20}H_{23}NOS$: C 73.81, H 7.12, N 4.30; found C 73.42, H 7.52, N 4.03%.

2.1.3. (1-Cyano-2-{5-[2-(1,2,2,4-tetramethyl-1,2,3,4-tetrahydro-quinolin-6-yl)-vinyl]-thiophen-2-yl}-vinyl)-phosphonic acid dithyl ester (**QTCP**)

To a solution of **QTC** (65 mg, 0.2 mmol) and diethyl cyanomethyl-phosphonate (43 mg, 0.24 mmol) in 5 mL acetonitrile, 5 drop of piperidine was added. The reaction mixture was heated to reflux for 2 h under N_2. After removing of solvent the residue was column chromatographied (silica gel, CH_2Cl_2/EtOAc = 10:1 as eluent) to give a dark solid (75 mg, 78%). Mp 112–113 °C. ^1H NMR (Acetone-d_6, 400 MHz, ppm): δ 1.24 (s, 3H), 1.33 (s, 3H), 1.34–1.39 (m, 9H), 1.47 (dd, $J_1 = 12.9$ Hz, $J_2 = 13.0$ Hz, 1H), 1.87 (dd, $J_1 = 4.4$ Hz, $J_2 = 13.1$ Hz, 1H), 2.80–2.89 (m, 4H), 4.14–4.21 (m, 4H), 6.60 (d, $J = 8.5$ Hz, 1H), 7.24–7.25 (m, 3H), 7.37 (d, $J = 8.5$ Hz, 1H), 7.44 (s, 1H), 7.79 (d, $J = 4.0$ Hz, 1H), 8.03 (d, $J = 19.2$ Hz, 1H); HRMS-EI (*m/z*): $[M]^+$ calcd for $C_{26}H_{33}N_2O_3PS$, 484.1949; found, 484.1953; IR (KBr, cm^{-1}): 2202 (—CN); Anal. calcd for $C_{26}H_{33}N_2O_3PS \cdot 2CH_2Cl_2$: C 48.18, H 4.89, N 4.68; found C 47.86, H 5.32, N 4.83.

2.2. Measurements

All the used solvents for spectral measurements were of spectroscopic grade from Aldrich and used as received. The following abbreviations are used throughout the text: *n*-hexane, HEX; diethylether, DEE; dichloromethane, DCM; acetone, ACE; dimethylformamide, DMF; acetonitrile, ACN; and methanol, MeOH. The absorption and fluorescence spectra were measured on a HP-8453 spectrophotometer and a PTI-C-700 fluorescence spectrometer, respectively. The fluorescence quantum yields were determined by the relative method using optically matched solutions. Quinine sulfate in 1 N sulfuric acid ($\Phi_f = 0.546$ at 25 °C) was used as the standard [37]. The accuracy of the quantum yields reported here was expected to be better than ±10%. Fluorescence lifetimes were determined on a Chronos fluorescence lifetime spectrometer (ISS Champagn; IL, USA) and the excitation wavelength for all samples is 436 nm. In all experiments except for fluorescence quantum yield measurements, 2×10^{-5} M solutions were used and handled under dim light at 25 °C. The ^1H NMR spectra were recorded on a VARIAN INOVA 400 MHz NMR spectrometer. MS spectra were measured on a GCT CA156 High Resolution Mass Spectrometer (HRMS). Elemental analyses were performed on a Thermoquest-Flash EA 1112 elemental analyzer. IR spectra were recorded on a JASCO FT/IR 430 spectrophotometer as KBr discs.

2.3. Calculation details

All the ground-state geometrical structures were fully optimized at B3LYP [38] level with the 6-31G(d,p) basis set using the GAUSSIAN 03 program package [39]. While the excited-state geometries were optimized using the time-dependent density functional theory (TDDFT) method with the TURBOMOLE program packages [40]. In the geometrical optimization of the low-lying electronically excited states, the B3LYP functional and the basis set of triple-ζ valence quality with one set of polarization functions (TZVP) were used [38,41]. Moreover, fine quadrature grids of size 4 were employed.

3. Results and discussion

3.1. Electronic spectra

Strong solvatochromism is a widely used criterion to identify a charge-transfer state [42], such as for several thiophene D–A compounds where absorption and emission bands were reported [34,43–48]. The absorption and fluorescence spectra of **QTC** and **QTCP** have been studied in different solvents and the experimental results are summarized in Table 1. The absorption spectra of these two compounds in selected solvents such as HEX and ACN are presented in Fig. 1. The absorption spectra consist of a strong absorption band in the visible region and a relatively weak shoulder in the near UV region. It is found that the position of the higher energy absorption peak is almost independent on solvent polarity and this band should be assigned to the π–π* transition. Due to the strong push–pull systems, red shifts of the lower energy absorption band in polar solvent indicate that this band could be attributed to the electronic transition delocalized throughout the whole molecule with a charge-transfer character, which is consistent with the assignment to the transition from the ground state (S_0) to the first singlet excited state (S_1) according to calculation results (see Section 3.4). Comparison of the spectra of **QTC** and **QTCP** obtained in solvents with different polarity, both **QTC** and **QTCP** show broadened absorption bands with long wavelength tail in more polar solvent, such as ACN. These tails seem to originate from the ground-state CT interaction between the donor and acceptor moieties [49].

Fig. 2a and b shows the fluorescence spectra of **QTC** and **QTCP** in some selected solvents with various polarities at room temperature. These two compounds exhibit altered fluorescence spectra in different solvents, either by a change in the relative intensity of vibrational bands or by a shift in the positions of the emitting bands. In non-polar solvent

Table 1
Maxima of UV–vis absorption (λ_{abs}), fluorescence (λ_{f}), Stokes shifts ($\Delta\nu_{st}$), fluorescence quantum yields (Φ_{f}) and lifetimes (τ) of **QTC** and **QTCP** in different solvents

	Solvents	λ_{abs}/nm	λ_{f}[a]/nm	$\Delta\nu_{st}$[b]/cm^{-1}	Φ_{f}	τ_{1}[c]/ns	τ_{2}[c]/ns
QTC	HEX	425	474(501)	2432	0.066	0.26(84)	3.4(16)
	DEE	432	533	4386	0.069	0.43(81)	3.2(19)
	DCM	453	601	5436	0.143	1.3(64)	3.2(36)
	ACE	442	603	6041	0.160	1.4(66)	3.5(34)
	MeCN	444	627	6574	0.146	1.6(64)	3.5(36)
	DMF	449	618	6090	0.142	1.6(42)	3.4(58)
	MeOH	448	666	7306	0.015	0.25(79)	2.8(21)
QTCP	HEX	473	544(583)	2759	0.144	0.65(75)	3.2(25)
	DEE	486	623	4525	0.249	1.73(66)	3.6(34)
	DCM	509	687	5090	0.181	2.9(90)	6.3(10)
	ACE	500	697	5653	0.099	2.4(86)	5.3(14)
	MeCN	500	721	6130	0.050	1.4(80)	3.9(20)
	DMF	511	718	5642	0.048	1.7(79)	4.3(21)
	MeOH	507	734	6100	0.022	0.42(75)	2.8(25)

[a] The second vibronic band is given in parentheses.

[b] $\Delta\nu_{st} = \nu_{abs} - \nu_{f}$.

[c] Lifetimes were measured after excitation at 436 nm and use fluorescein ($\tau = 4$ ns) as reference, relative contributions are shown in parentheses.

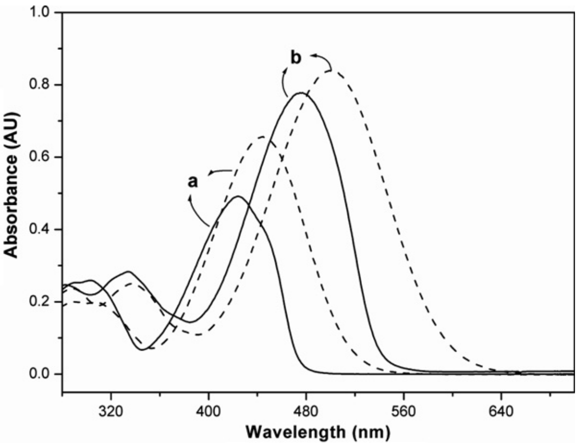

Fig. 1. UV–vis absorption of **QTC** (a) and **QTCP** (b) in hexane (solid line) and acetonitrile (dashed line) solutions (2×10^{-5} M).

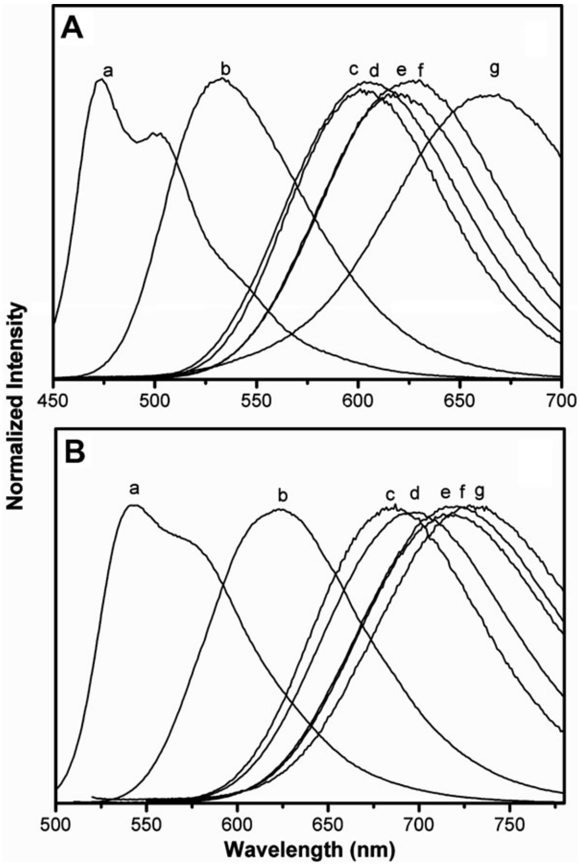

Fig. 2. The fluorescence spectra of (A) **QTC** and (B) **QTCP** in (a) HEX, (b) DEE, (c) DCM, (d) ACE, (e) DMF, (f) ACN and (g) MeOH.

such as HEX, the fluorescence spectra of **QTC** and **QTCP** exhibit vibrational structures, which indicates two separated close-lying excited states. The weak solute–solvent interactions in this non-polar medium that do not broaden the vibronic transition too much should be responsible for this observation. When the polarity and the hydrogen-bonding power of the solvent increases, the fluorescence is structureless and exhibits a solvatochromic red-shift due to the dipole–dipole interactions between the solute and solvents [50]. The maxima of fluorescence band significantly shift to low energy in polar solvents, indicating a strong ICT character for the excited state [51]. For example, the fluorescence spectra maxima of **QTC** show a remarkable positive solvatochromism of 153 nm red-shift from HEX to ACN. And a more red-shifted value of 192 nm was observed when compare the fluorescence maxima between HEX and MeOH. The hydrogen-bonding effect of MeOH on the chromophore, which stabilized the charge-separated excited state, should be the reason for this larger red-shift for the fluorescence maxima [43]. As a result of fluorescent positive solvatochromism, the Stokes shifts increase with increasing of the polarity of solvent pointing to large solvent relaxation and stronger stabilization of the excited state in polar solvents. So-large difference of the Stokes shifts between non-polar (HEX) and polar solvents (such as ACN) suggests that the fluorescent emissions may be originated from different excited-state geometries in different solvents. Therefore, it can be expected that an excited state with the twisted geometry, which may be induced by the polarity of solvents, takes place after photoexcitation of these thiophene-π-conjugated donor–acceptor systems.

3.2. Solvatochromic measurements: excited-state dipole moment (μ_e) of **QTC** and **QTCP**

From standard steady-state solvatochromic shift measurements, a Lippert–Mataga methodology was used to determine the excited-state dipole moment (μ_e). Fig. 3 shows the plot of fluorescent emission maxima energy (v_f) of **QTC** and **QTCP** versus the different solvent parameter (Δf). The dipole moment of the excited state (μ_e) can be estimated from the slope of the plot according to Eq. (1) [51–53]:

$$v_f = -[(1/4\pi\varepsilon_0)(2/hca^3)][\mu_e(\mu_e - \mu_g)]\Delta f + \text{Const.} \quad (1)$$

where

$$\Delta f = (\varepsilon - 1)/(2\varepsilon + 1) - 0.5(n^2 - 1)/(2n^2 + 1) \quad (2)$$

and

$$a = (3M/4N\pi d)^{1/3} \quad (3)$$

where v_f is the fluorescent emission maxima energy, h is Planck's constant, c is the speed of light, μ_g is the ground-state dipole moment and estimated at the B3LYP level with the 6-31G(d,p) basis set using the GAUSSIAN 03 program package, a is the solvent cavity (Onsager) radius, which could be derived from the Avogadro number (N), molecular weight (M), and density (d). Where ε, ε_0, and n are the solvent dielectric, vacuum permittivity, and the solvent refractive index, respectively.

From the slope of the plot in Fig. 3, the excited-state dipole moments μ_e of 23.7 D is obtained by adopting the ground-state dipole moment μ_g of 11.23 D for **QTCP**. In the case of **QTC**, the corresponding μ_e and μ_g values are 21.2 D and 10.14 D, respectively. The large change in dipole moments between the excited state and the ground state supports the fact that an ICT process occurs through the excitation from ground state to excited state.

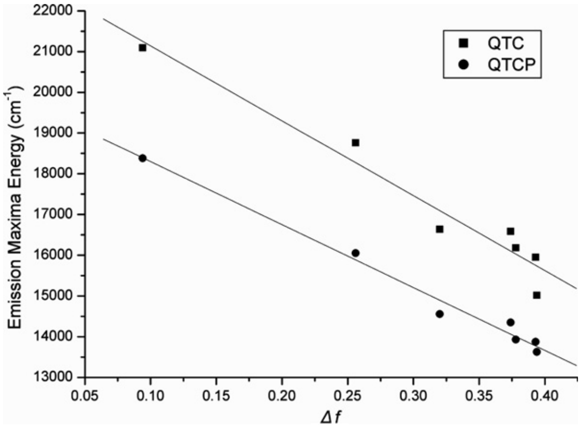

Fig. 3. Fluorescent emission maxima energy (v_f) as a function for the solvent parameter (Δf) of compound **QTC** and **QTCP**. Solvents are shown in Table 1.

3.3. Fluorescence quantum yields and lifetimes

The fluorescence quantum yields for **QTC** and **QTCP** in different solvents have been determined and the data are also collected in Table 1. The relationship between the Φ_f and the solvent polarity expressed as $E_T(30)$ [54] is shown in Fig. 4. All of these two compounds are strongly fluorescent in the solvent of middle polarity, such as **QTC** in ACE and **QTCP** in DEE, and the values of Φ_f decrease in more polar solvents. The reduction in Φ_f from ACE or DEE to ACN can be attributed to the strong ICT interaction, however, the dramatic decrease of Φ_f in highly polar hydrogen bond donor solvent (MeOH) is the result of hydrogen-bonding interaction which enhanced non-radiative quenching of the fluorescence [55]. As shown in Fig. 4, the sigmodial curves in the plots of Φ_f against $E_T(30)$ are analogous to the acid–base titration curves, which indicates that the "equivalent point" of the population of molecules in a different excited-state structural geometry is achieved in solvents more polar than ACE for **QTC** and DEE for **QTCP** [51].

Further more, the fluorescence lifetimes (τ) of these compounds in different solvents were obtained and the data are also summarized in Table 1. The fluorescence decays are well fitted by biexponential functions and two different lifetimes (τ_1 and τ_2) with different contributions are observed in all these cases. It is expected that the two lifetimes be originated in the different radiative processes from the excited state to the different ground states with different geometries, such as *cis*- and *trans*-isomeric geometries. And thus a twisted geometry is also suggested for the excited

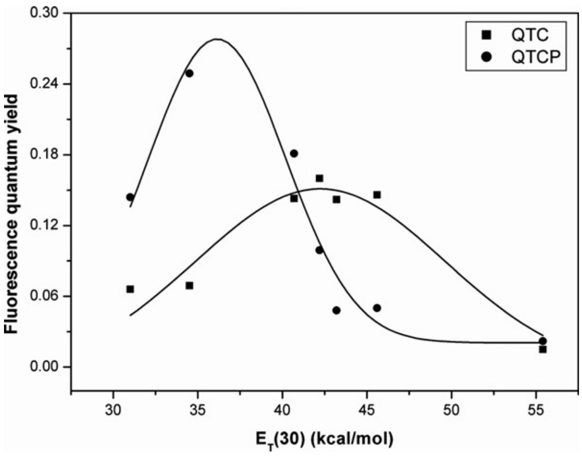

Fig. 4. Variation of the fluorescence quantum yields of **QTC** and **QTCP** with the solvent polarity. The solvents [$E_T(30)$] are (from lest to right) HEX [31.0], DEE [34.5], DCM [40.7], ACE [42.2], DMF [43.2], ACN [45.6] and MeOH [55.4].

state. The shorten lifetimes (τ_1) for **QTC** and **QTCP** show strong dependent on the solvent polarity and nearly the same trend to Φ_f values, indicating a strong interaction between the deactivation process with solvents. This shorter lifetime might be originated in the deactivation to the *trans*-isomer, as the *trans*-isomer has a larger dipole moment than the *cis*-isomer and also stronger interaction with solvents. The contribution values for τ_1 are always larger than that of τ_2 also suggest that this shorten lifetime should be the result of this deactivation process because *trans*-isomer is usually the stable isomer. The longer lifetimes (τ_2) are nearly solvent-independent for **QTC** but they show dependence with solvents for **QTCP**. The stronger push–pull system for **QTCP** results in the larger ground-state dipole moment for *cis*-isomer and thus, has stronger interaction with solvents might interpret this phenomenon.

3.4. Theoretical analysis of the ground and excited states

In the investigation of ICT of D-π-A systems, the molecular structure of the ICT states is an important point of discussion [21]. Herein, theoretical calculations were performed to study both the ground- and excited-state structures of **QTC** and **QTCP**. The geometrical structures of ground state and excited state at different conformations were fully optimized without any geometrical constrain. It is noted that the optimized geometries of these compounds yield fully planar geometry in the ground state (Fig. 5). While for the excited state, the optimized structures of the relaxed ICT state with perpendicular geometrical conformations are obtained. As shown in Fig. 5, the optimized lowest energy structure of the ICT state is suggested to be a twisted geometry with distorted C=C double bond between the donor moiety (TMTHQ) and the thiophene-π-bridge in both compounds.

Frontier molecular orbitals (MOs) of the **QTC** and **QTCP** at planar and perpendicular geometries are shown in Fig. 6. The first and second singlet excited states (S_1 and S_2) mainly correspond with the HOMO → LUMO and HOMO-1 → LUMO transitions, respectively, according to the analysis of orbital transition. Both of the electron densities of HOMO and LUMO are delocalized over the molecules at the planar ground-state geometries of **QTC** and **QTCP**. As the optimized lowest energy structures of these compounds are twisted geometries, much attention should be paid to the electron density distribution of LUMO in the twisted excited state. For the twisted conformation for **QTC** and **QTCP**, the electron densities of LUMO orbitals are distinctly separated. We can find that the electron density of LUMO is localized on the electron-withdrawing moiety. Therefore, the HOMO–LUMO electronic promotion can be identified as the ICT transition at the twisted conformations [56–59]. While for the HOMO-1 → LUMO transition, it is evident that S_2 state is of π–π* character from Fig. 6. From the analysis of frontier molecular orbitals, the ICT character for the S_1 states of the thiophene-π-conjugated compounds **QTC** and **QTCP** is confirmed.

In Table 2, the calculated absorption and fluorescence electronic excitation energies and the corresponding assignment for the planar and twisted **QTC** and **QTCP** are presented. It shows that the calculated absorption maximum excitation energies (S_1, 2.805 eV for **QTC** and 2.495 eV for **QTCP**) are in good agreement with the experimental absorption values. However, the calculated S_2 excitation

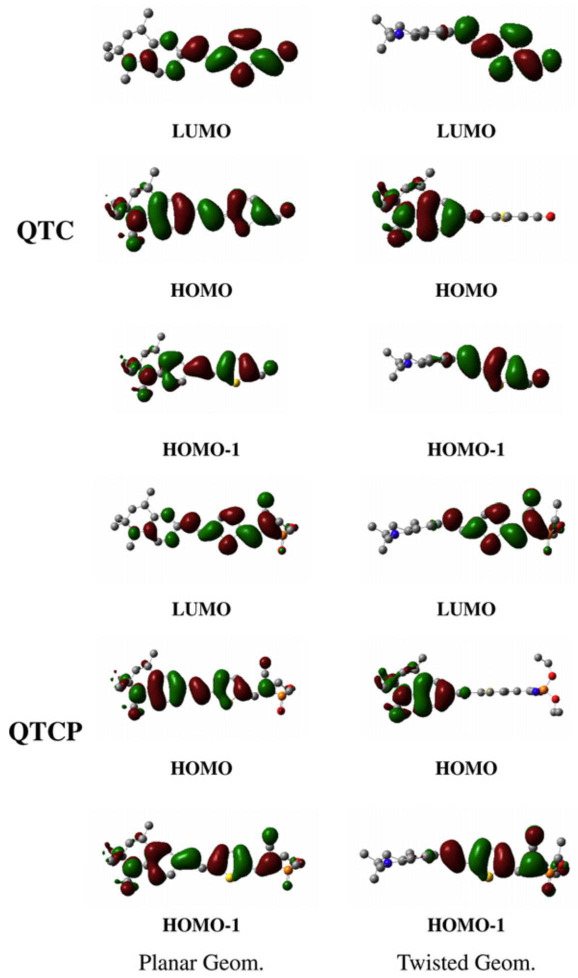

Fig. 6. The frontier molecular orbitals (MOs) for the planar and twisted geometrical structures of **QTC** and **QTCP**.

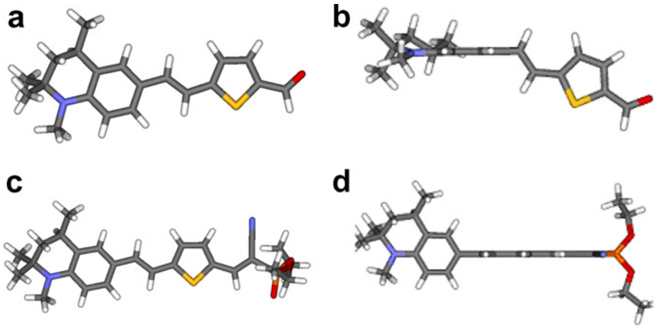

Fig. 5. The optimized lowest energy structures of the ground (a, c) and ICT (b, d) states of **QTC** (a, b) and **QTCP** (c, d).

Table 2
Calculated absorption and fluorescence electronic excitation energies (eV) and corresponding assignment (in the parenthesis) for **QTC** and **QTCP**

	QTC		**QTCP**	
	Planar	Twisted	Planar	Twisted
Absorption				
S_1	2.805(H → L)	–	2.495(H → L)	–
S_2	3.523(H-1 → L)	–	3.416(H-1 → L)	–
Fluorescence				
S_1	2.684	2.112	2.380	1.769

energies are some different with the experimental results. From the calculated total energies of the molecules at different geometric structures, it is clear that both **QTC** and **QTCP** in the equilibrium ground states prefer to the planar geometrical conformations. Furthermore, by comparison with the calculated and experimental fluorescence emission energies, one can see that the fluorescence of **QTC** and **QTCP** in non-polar solvents are more like emitted from the excited states at the planar geometric conformations while in polar solvents are emitted from the excited states at the twisted geometric conformations [13]. So solvents play an important role for the S_1 fluorescence of **QTC** and **QTCP** in solution. In the S_1 fluorescence state, the polarity of solvents can induce the ICT progress followed the geometric twisting.

The Mulliken population analysis of the ground and excited states indicates a significant charge-separated character between the donor and acceptor moieties in the excited state. For **QTCP**, the net charge of TMTHQ moiety in ground state is 0.1585. In the final twisted exited state, the net charge of the donor moiety increases to 0.7011 upon photoexcitation. As for **QTC**, the Mulliken net charge for the TMTHQ moiety increases by 0.7741 in the twisted ICT state as compared to that in the ground state. The drastic charge changes for **QTC** and **QTCP** in S_1 state indicate that the excited state possesses considerable ICT character.

4. Conclusion

In conclusion, compounds **QTC** and **QTCP** have been designed and synthesized as novel thiophene-π-conjugated donor–acceptor molecules. Combined experimental and theoretical methods have been performed to investigate the photoinduced ICT processes of these compounds. Steady-state absorption and fluorescence measurements in different solvents indicate the photoinduced ICT characters of **QTC** and **QTCP**. Solvent dependency of the large Stokes shift and high dipole moment of the excited state also support charge-transfer character of the excited state. TDDFT calculations were performed to study the ground and excited-state geometrical structures. The results reveal that the excited state has adopted a distortion of the C=C double bond between the donor moiety and the thiophene-π-bridge. Analysis of molecular orbitals and Mulliken populations for **QTC** and **QTCP** indicates a significant charge separation character between the donor and acceptor moieties in the excited state.

Acknowledgements

This work was supported by the Programme of Introducing Talents of Discipline to Universities. We also acknowledge the National Natural Science Foundation of China (No. 20633020), the Ministry of Science and Technology (MOST), Ministry of Education (MOE), the Swedish Energy Agency and the Swedish Research Council for their financial support.

References

[1] B.J. Coe, J.A. Harris, B.S. Brunschwig, J. Garin, J. Orduna, S.J. Coles, M.B. Hursthouse, J. Am. Chem. Soc. 126 (2004) 10418.
[2] P.R. Varanasi, A.K.-Y. Jen, J. Chandrasekhar, I.N.N. Namboothiri, A. Rathna, J. Am. Chem. Soc. 118 (1996) 12443.
[3] R.Y. Lai, X. Kong, S.A. Jenekhe, A.J. Bard, J. Am. Chem. Soc. 126 (2003) 12631.
[4] C.-Y. Chen, J.-H. Ho, S.-L. Wang, T.-I. Ho, Photochem. Photobiol. Sci. 2 (2003) 1232.
[5] A.W. Czarnik, Acc. Chem. Res. 27 (1994) 302.
[6] K.A. Willets, P.R. Callis, W.E. Moerner, J. Phys. Chem. B 108 (2004) 10465.
[7] T. Kitamura, M. Ikeda, K. Shigaki, T. Inoue, N.A. Anderson, X. Ai, T. Lian, S. Yanagida, Chem. Mater. 16 (2004) 1806.
[8] S. Delmond, J.-F. Létard, R. Lapouyade, W. Rettig, J. Photochem. Photobiol. A 105 (1997) 135.
[9] W. Ma, Y. Wu, J. Han, D. Gu, F. Gan, J. Mol. Struct. 752 (2005) 9.
[10] E. Lippert, W. Lűder, F. Moll, W. Nägele, H. Boos, H. Prigge, I. Seibold-Blankenstein, Angew. Chem. 73 (1961) 695.
[11] E. Lippert, W. Lűder, H. Boos, in: A. Mangini (Ed.), Advances in Molecular Spectroscopy, Pergamon Press, Oxford, 1962, pp. 443–457.
[12] W. Rettig, Angew. Chem. Int. Ed. Engl. 25 (1986) 971.
[13] Z.R. Grabowski, K. Rotkiewicz, W. Rettig, Chem. Rev. 103 (2003) 3899.
[14] W. Rettig, B. Bliss, K. Dirnberger, Chem. Phys. Lett. 305 (1999) 8.
[15] W. Rettig, B. Zietz, Chem. Phys. Lett. 317 (2000) 187.
[16] B. Mennucci, A. Toniolo, J. Tomasi, J. Am. Chem. Soc. 122 (2000) 10621.
[17] D. Rappoport, F. Furche, J. Am. Chem. Soc. 126 (2004) 1277.
[18] A. Köhn, C. Hättig, J. Am. Chem. Soc. 126 (2004) 7399.
[19] K.A. Zachariasse, M. Grobys, Th. von der Haar, A. Hebecker, Y.V. Il'ichev, O. Morawski, I. Rückert, W. Kühnle, J. Photochem. Photobiol. A 105 (1997) 373.
[20] K.A. Zachariasse, Chem. Phys. Lett. 320 (2000) 8.
[21] K.A. Zachariasse, S.I. Druzhinin, W. Bosch, R. Machinek, J. Am. Chem. Soc. 126 (2004) 1705.
[22] E. Martín, J.L.Gu. Coronado, J.J. Camacho, A. Pardo, J. Photochem. Photobiol. A 175 (2005) 1.
[23] A. Amini, A. Harriman, J. Photochem. Photobiol. C 4 (2003) 155.
[24] C.J. Jödicke, H.P. Lüthi, J. Am. Chem. Soc. 125 (2003) 252.
[25] A. Chakraborty, S. Kar, N. Guchhait, J. Photochem. Photobiol. A 181 (2006) 246.
[26] S. Techert, K.A. Zachariasse, J. Am. Chem. Soc. 126 (2004) 5993.
[27] H. Ishikawa, M. Sugiyama, I. Baba, W. Setaka, M. Kira, N. Mikami, J. Phys. Chem. A 109 (2005) 8959.
[28] J. Laane, Int. Rev. Phys. Chem. 18 (1999) 301.
[29] J. Laane, J. Phys. Chem. A 104 (2000) 7715.
[30] M.C. Ruiz Delgado, V. Hernández, J. Casado, J.T. López Navarrete, J.-M. Raimundo, P. Blanchard, J. Roncali, J. Mol. Struct. 651–653 (2003) 151.

[31] M.C. Ruiz Delgado, V. Hernández, J. Casado, J.T. López Navarrete, J.-M. Raimundo, P. Blanchard, J. Roncali, J. Mol. Struct. (THEOCHEM) 709 (2004) 187.
[32] M.C. Ruiz Delgado, V. Hernández, J. Casado, J.T. López Navarrete, J.-M. Raimundo, P. Blanchard, J. Roncali, Chem. Eur. J. 9 (2003) 3670.
[33] M.Yu. Krysin, Kh.S. Shikhaliev, I.K. Anokhina, Zh.V. Shmyreva, Chem. Heterocycl. Compd. 37 (2001) 227.
[34] A.K.-Y. Jen, V.P. Rao, K.Y. Wong, K.J. Drost, J. Chem. Soc. Chem. Commun. (1993) 90.
[35] X. Yang, X. Jiang, C. Zhao, R. Chen, P. Qin, L. Sun, Tetrahedron Lett. 47 (2006) 4961.
[36] D. Craig, J. Am. Chem. Soc. 60 (1938) 1458.
[37] J.N. Demas, G.A. Grosby, J. Phys. Chem. 75 (1971) 991.
[38] A.D. Becke, J. Chem. Phys. 98 (1993) 5648.
[39] M.J. Frisch et al., Gaussian 03, Revision B.05, Gaussian, Inc., Pittsburgh, PA, 2003.
[40] R. Ahlrichs et al., Turbomole 5.7.1, the Quantum Chemistry Group, University of Karlsruhe, Germany, 2005.
[41] A. Schäfer, C. Huber, R. Ahlrichs, J. Chem. Phys. 100 (1994) 5829.
[42] N. Acar, J. Kurzawa, N. Fritz, A. Stockmann, C. Roman, S. Schneider, T. Clark, J. Phys. Chem. A 107 (2003) 9530.
[43] S.-L. Wang, T.-I. Ho, J. Photochem. Photobiol. A 135 (2000) 119.
[44] P. Garcia, J.M. Pernaut, P. Hapiot, V. Wintgens, P. Valat, F. Garnier, D. Delabouglise, J. Phys. Chem. 97 (1993) 513.
[45] W. Rettig, V. Kharlanov, F. Effenberger, F. Steybe, Chem. Phys. Lett. 404 (2005) 272.
[46] J. Casado, L.L. Miller, K.R. Mann, T.M. Pappenfus, H. Higuchi, E. Ortí, B. Milián, R. Pou-Amérigo, V. Hernández, J.T.L. Navarrete, J. Am. Chem. Soc. 124 (2002) 12380.
[47] B. Milián, E. Ortí, V. Hernández, J.T.L. Navarrete, T. Otsubo, J. Phys. Chem. B 107 (2003) 12175.
[48] J. Casado, T.M. Pappenfus, K.R. Mann, B. Milián, E. Ortí, P.M. Viruela, M.C.R. Delgado, V. Hernández, J.T.L. Navarrete, J. Mol. Sturct. 651 (2003) 665.
[49] M. Maiti, T. Misra, T. Bhattacharya, C. Basu (nee Deb), A. De, S.K. Sarkar, T. Ganguly, J. Photochem. Photobiol. A 152 (2002) 41.
[50] M. Maus, W. Rettig, D. Bonafoux, R. Lapouyade, J. Phys. Chem. A 103 (1999) 3388.
[51] J.-S. Yang, K.-L. Liau, C.-M. Wang, C.-Y. Hwang, J. Am. Chem. Soc. 126 (2004) 12325.
[52] E.Z. Lippert, Elecktrochem 61 (1957) 962.
[53] N. Mataga, Y. Kaifu, M. Koizumi, Bull. Chem. Soc. Jpn. 29 (1956) 465.
[54] C. Reichardt, Chem. Rev. 94 (1994) 2319.
[55] T.A. Fayed, Chem. Phys. 324 (2006) 631.
[56] M. Sun, J. Chem. Phys. 124 (2006) 054903.
[57] M. Sun, Int. J. Quantum Chem. 106 (2006) 1020.
[58] E. Fabiano, F. Della Sala, R. Cingolani, M. Weimer, A. Görling, J. Phys. Chem. A 109 (2005) 3078.
[59] G. Zhao, K. Han, J. Phys. Chem. A 111 (2007) 2469.